ELSEVIER

Neuroscience Letters 218 (1996) 185–187

NEUROSCIENCE LETTERS

Analytical characterization of spontaneous activity evolution during hippocampal development in the rabbit

Liset Menendez de la Prida, Sonia Bolea, Juan V. Sanchez-Andres*

Departamento de Fisiología, Instituto de Neurociencias, Universidad de Alicante, Campus de San Juan, aptdo. 374, Alicante 03080, Spain

Received 12 June 1996; revised version received 12 September 1996; accepted 19 September 1996

Abstract

We have analyzed the postnatal evolution of the spontaneous electrical activity in pyramidal neurons from rabbit hippocampal slices. The firing mode of CA1 neurons changes from bursting to regular spiking along the first postnatal month. Interspike intervals (ISIs) were used to account for the dynamical structure of the firing behavior. Histograms and joint interval scattergrams show that the firing mode from (P0–P7) cells has a different distribution from that obtained in (P15–P25) neurons. We have used a mathematical measure called the product of inertia to quantify this difference. Our findings demonstrate that the spontaneous activity changes along the maturational process.

Keywords: Slices; Postnatal development; Intracellular recording; Interspike intervals; Bursting; Firing patterns

In rodents, the first postnatal month is a specially active temporal window. During this period, the hippocampal pyramidal neurons have small and long action potentials, the input resistance decreases and the membrane potential hyperpolarizes [7]. Patch-clamp studies have demonstrated variations of ionic currents like I_A [9] while several network mechanisms, such as the inhibitory system, are also changing [10]. Previous work has shown that bursting is a remarkable spontaneous event of CA3 neuronal activity, but specially accentuated in immature networks [2,10]. Nevertheless, neither the CA1 immature neuronal activity nor the electrical pattern that follows bursting disappearance have been characterized. In this paper we analyze the normal evolution of CA1 spontaneous activity, looking for observable changes of the maturational process.

Intracellular recordings were obtained in 500 μm hippocampal slices from New Zealand white rabbits (0–25 postnatal days, $n = 68$ cells). The slices were prepared as previously described [6]. Borosilicate electrodes were filled with 3 M KCl (resistance, 50–100 MΩ). The impalements were made at the CA1 stratum pyramidale. The criteria for a healthy cell were: membrane potentials greater than –50 mV, spike train response to positive current injection, overshooting action potentials and input resistance larger than 20 MΩ [7]. The possibility of immature neuron injury is ruled out since the newborn recorded cells have a mean input resistance of about 69 MΩ. Values are given as mean ± SD. Significance analysis using Student's two-tailed *t*-test (confidence level, $P = 0.05$) were applied.

The records in Fig. 1A,C show different spontaneous firing patterns at two stages of CA1 postnatal maturation. Bursting in the form of giant depolarizing potentials (GDPs) is frequent during the first week (Fig. 1A) in agreement with previous studies in CA3 [2,10]. The GDPs (Fig. 1B1) have a mean amplitude of 21 ± 4 mV, a duration from 190 to 750 ms and are crowned by 2–6 spikes (92 GDPs, $n = 21$ cells). They were blocked by bicuculline and have a reversal potential of –26 ± 2 mV ($n = 4$, data not shown) according with previous reports obtained with KCl filled electrodes [2]. Spontaneous interictal discharges (Fig. 1B2) have been also detected around the second week as previously reported [3], but we have not separated these two events since for our purpose both of them can be considered as bursts.

After the second week bursting tends to disappear (Fig. 1C). We quantified the experimental progression by look-

* Corresponding author. Tel.: +34 6 5659811, ext. 277; fax: +34 6 5658539; e-mail: jv@juanvi.fisi.ua.es

PII S0304-3940(96)13095-0

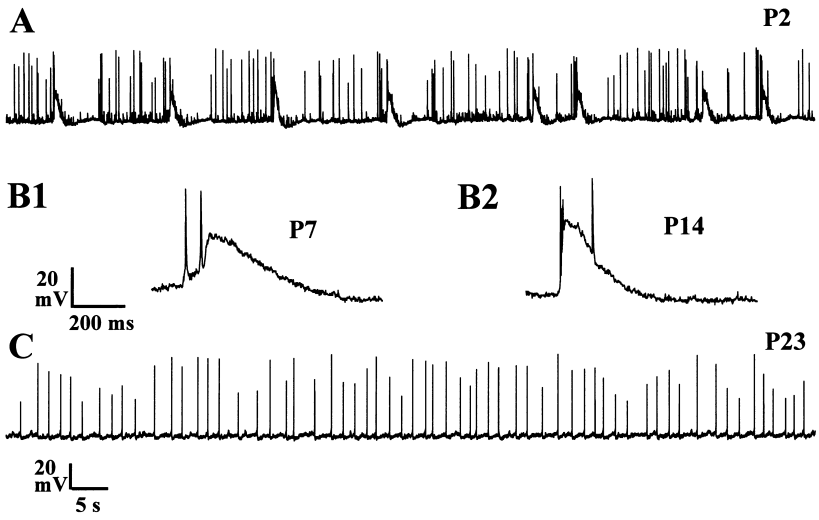

Fig. 1. Changes in the spontaneous electrical activity of CA1 pyramidal neurons along postnatal development. (A) Bursting behavior present in the first postnatal week. (B1) A typical GDP from a P7 subject. (B2) An example of interictal discharge recorded in the second week of life. (C) Regular spiking is present in the third week. Calibration bars are common for (A,C) (B1,B2). Records were filtered at 1 KHz.

ing at the number of spontaneous bursts/min (Fig. 2). There is a clear tendency towards a reduction of bursting as maturation proceeds. Large errors in (P0–P10) are a manifestation of the heterogeneity of the developmental course. Based on this result we have selected two groups from the extremes of the maturational process. The first group is integrated by the cells from P0 to P7, they showed the greatest values of bursting frequency. The cells from the second group (P15–P25) fire in a different mode characterized by a regular spiking.

To analyze the firing pattern, interspike intervals (ISIs) were computed. ISIs have been extensively used to characterize electrophysiological data [1,4]. The frequency histograms of ISIs clearly demonstrate the different firing modes of these two groups. Fig. 3 shows the results from a sample of eight cells for each case. They are all presented in one single graph, so the final frequency count is obtained by the addition of each frequency count from the eight different histograms from each group. A clear feature is that the more immature group (P0–P7) has a peak at short intervals (Fig. 3A) while (P15–P25) show a unimodal distribution centered around 1.15 ± 0.21 s (Fig. 3B). Computation of the median confirms this difference. For (P0–P7) we obtain a value of 0.067 ± 0.008 s ($n = 10$) which is significantly different from the value of the second group, 1.296 ± 0.071 s ($n = 10$); ($t = 10.50$, $P = 0.00015$).

Although it is clear that cells from the two groups fired in a different fashion, the previous statistic analysis do not provide an adequate tool to quantify the distributions. In a recent paper Rapp et al. [4] introduced a measure called

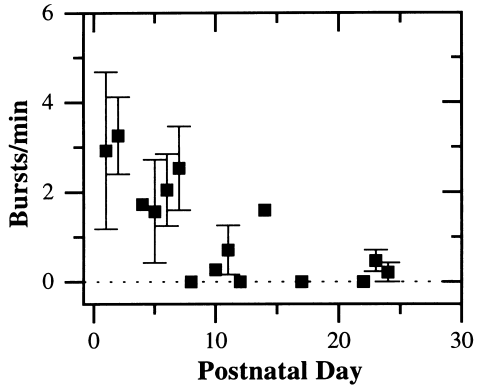

Fig. 2. Quantification of the number of bursts along development. Points without error bars are single data for the corresponding postnatal ages, except those of zero bursts/min that do not have SD.

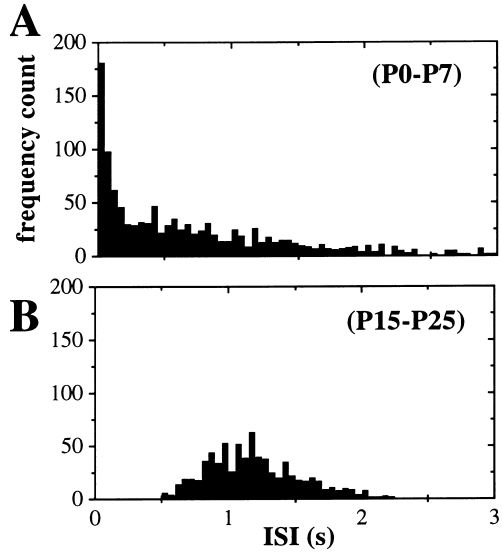

Fig. 3. Frequency histograms from the two groups (P0–P7), (P15–P25). Each graph summarizes the results obtained from a sample of eight cells from each group. (A) The cells from P0–P7 show a pronounced peak at short time intervals (0–100 ms). (B) Regular spiking from (P15–P25) have a typical unimodal distribution centered around 1.15 s.

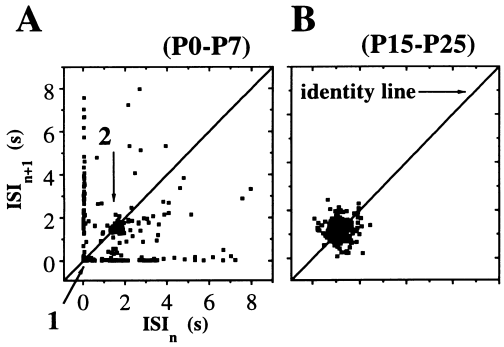

Fig. 4. Joint interval scattergrams along early postnatal development. (A) Scattergrams from $n = 3$ (P0–P7) cells are superimposed. The bursting behavior of these neurons have a typical square-shaped distribution [8] which is characterized by two clusters in the identity line ($ISI_n = ISI_{n+1}$). Cluster 1 (see arrow 1) is formed by the consecutive spikes that crown the depolarizing potential of each burst. A second cluster (arrow 2) is integrated by the spikes between the bursts. (B) Superposition of joint interval scattergrams from $n = 4$ (P15–P25) neurons. The regular spiking pattern from these cells is characterized by a single cluster on the identity line (see arrow).

product of inertia (P_2) that successfully identifies differences in firing patterns. To obtain this measure we plotted the pairs (ISI_n, ISI_{n+1}) building an scatter diagram called joint interval scattergram [5]. This type of diagram showed also evidence for the different firing characteristic of cells from the two groups (see Fig. 4 and caption).

To contrast these two firing patterns we compute the product of inertia. In the joint interval scattergrams P_2, is defined as

$$P_2 = -\sum_{i=1}^{N_p}\sum_{j=1}^{N_p}\left(\frac{i}{N_p}-\frac{i_{cm}}{N_p}\right)\cdot\left(\frac{j}{N_p}-\frac{j_{cm}}{N_p}\right)\cdot p_{ij}$$

where N_p is the number of intervals in which each axis is partitioned and p_{ij} denotes the probability density in each partition (i, j). Here (i_{cm}, j_{cm}) denotes the coordinate of the center of mass of the distribution in the scattergram

$$i_{cm} = \sum_{i=1}^{N_p}\sum_{j=1}^{N_p} i\cdot p_{ij}, \text{idem for } j_{cm} \text{ substituting } i \text{ by } j.$$

Thus P_2 gives a measure of the distance between pairs and the center of mass. We have used $N_P = 200$, and in all cases the asymptotic behavior for larger N_p was corroborated.

Computation of P_2 confirms the difference between the firing patterns. The mean value of P_2 in (P0–P7) was -0.0029 ± 0.0001 ($n = 10$) which is highly significantly different ($t = 6.17$, $P = 0.001$) from (P15–P25), $(-7.10 \pm 0.2)\cdot 10^{-5}$ ($n = 10$). Since P_2 computes the distance between the pairs and the center of mass, it is reasonable to expect extremely low values for the unimodal distribution. Intuitively, in this case the coordinate of mean value should lay near to the center of mass in contrast with the bursting distribution.

In summary, we have found that CA1 pyramidal cells from P0–P7 show a quite different firing behavior when compared with (P15–P25) neurons. Specifically, these former show bursting activity while neurons from (P15–P25) fire in a regular fashion. Simple statistics show that the median from these two firing patterns are significantly different. Histograms, joint interval scattergrams and a theoretical measure such as the product of inertia, were used and confirmed such a difference.

After the second postnatal week the inhibitory system and several physiological and structural constants seems to be stabilized [2,7,10]. This is the time when spontaneous bursts have disappeared strengthening the view of its presence as a strict feature of CA1 immaturity. The analytical characterization presented here gives formal support to this fact, and encourage further experimental and theoretical studies.

This work was supported by grant PM92-0115 from DGYCIT. L.M.P. and S.B. were supported by Fellowships of GV and MEC respectively. We would like to thank N. Stollenwerk for helpful discussions, E. Geijo and R. Gallego for carefully reading of the manuscript and useful comments and A. Vergara and S. Moya for technical help.

[1] Bair, W., Koch, C., Newsome, W. and Britten, K., Power spectrum analysis of bursting cells in area MT in the behaving monkey, J. Neurosci., 14 (1994) 2870–2892.
[2] Ben-Ari, Y., Cherubini, E., Corradetti, R. and Gaiarsa, J.L., Giant synaptic potentials in immature rat CA3 hippocampal neurones, J. Physiol., 416 (1989) 303–325.
[3] Haglund, M.M. and Schwartzkroin, P.A., Seizure-like spreading depression in immature rabbit hippocampus in vitro, Brain Res., 316 (1984) 51–59.
[4] Rapp, P.E., Goldberg, G., Albano, A.M., Janicki, M.B., Murphy, D., Niemeyer, E. and Jimenez-Montaño, M.A., Using coarse-grained measures to characterize electromyographic signals, Int. J. Bifur. Chaos, 3 (1993) 525–541.
[5] Rodiek, R.W., Kian, N.Y. and Gerstein, G.L., Some quantitative methods for the study of spontaneous activity of single neurons, Biophys. J., 2 (1962) 351–368.
[6] Sanchez-Andres, J.V. and Alkon, D.L., Voltage-clamp analysis of the effects of classical conditioning on the hippocampus, J. Neurosci., 65 (1991) 796–807.
[7] Schwartzkroin, P.A., Development of rabbit hippocampus: physiology, Dev. Brain Res., 2 (1982) 469–486.
[8] Selz, K.A. and Mandell, A.J., Critical coherence and characteristic times in brainstem neuronal discharge patterns. In T. McKenna, J. Davis and S.F. Zornetzer (Eds.), Single Neuron Computation, Academic Press, New York, 1992, pp. 525–560.
[9] Spigelman, I., Zhang, L. and Carlen, P.L., Patch-clamp study of postnatal development of CA1 neurons in rat hippocampal slices: membrane excitability and K + currents, J. Neurophysiol., 68 (1992) 55–69.
[10] Swann, J.W., Smith, K.L. and Brady, R.J., Age-dependent alterations in the operations of hippocampal neural networks, Ann. N. Y. Acad. Sci., 627 (1991) 264–276.